MOLECULAR IMAGING AND BIOLOGY

Mol Imaging Biol (2019) 21:328–338
DOI: 10.1007/s11307-018-1244-5

Published Online: 28 June 2018

RESEARCH ARTICLE

Near-Infrared Spatially Resolved Spectroscopy as an Indirect Technique to Assess Brown Adipose Tissue in Young Women

Francisco M. Acosta,[1] Jörn Berchem,[1,2] Borja Martinez-Tellez,[1,3] Guillermo Sanchez-Delgado,[1] Juan M. A. Alcantara,[1] Lourdes Ortiz-Alvarez,[1] Takafumi Hamaoka,[4] Jonatan R. Ruiz[1]

[1]*PROFITH "PROmoting FITness and Health through physical activity" Research Group, Department of Physical and Sports Education, Faculty of Sports Science, University of Granada, Carretera de Alfacar, s/n, 18071, Granada, Spain*

[2]*Department of Sports Medicine, Institute of Sports Sciences, Justus-Liebig-University Giessen, Kugelberg 62, 35394, Giessen, Germany*

[3]*Department of Medicine, Division of Endocrinology, and Einthoven Laboratory for Experimental Vascular Medicine, Leiden University Medical Center, Leiden, The Netherlands*

[4]*Department of Sports Medicine for Health Promotion, Tokyo Medical University, 6-1-1, Shinjuku, Shinjuku-ku, Tokyo, 160-8402, Japan*

Abstract

Purpose: Near-infrared spectroscopy (NIRS) has recently been proposed as an indirect technique to assess brown adipose tissue (BAT) in young men. NIRS arises as a novel technique to avoid the limitations of the "gold-standard" 2-deoxy-2-[^{18}F]fluoro-D-glucose ([^{18}F]DG) positron emission tomography combined with X-ray computed tomography (PET/CT). The aim of this study was to examine the association between near-infrared spatially resolved spectroscopy (NIR_{SRS}) parameters and BAT volume and activity estimated by [^{18}F]DG-PET/CT in 18 young healthy women.

Procedures: NIR_{SRS} parameters [tissue saturation index and concentrations of total haemoglobin, oxy-haemoglobin, and deoxy-haemoglobin] were continuously measured in the supraclavicular and forearm regions, in both warm and cold (2 h of personalised cold exposure) conditions. Then, the NIR_{SRS} data were analysed as an average of 5 min in 4 different periods: (i) warm period as the baseline record, (ii) cold period I, (iii) cold period II, and (iv) cold period III. The data were then correlated with BAT volume and activity (SUV_{mean} and SUV_{peak}) estimated by [^{18}F]DG-PET/CT.

Results: There was no association between the NIR_{SRS} parameters in the supraclavicular region in warm conditions (no previous cold exposure) and BAT volume and activity ($P > 0.05$). Similarly, the cold-induced changes of the NIR_{SRS} parameters in the supraclavicular region were not associated with BAT volume and activity ($P > 0.05$).

Conclusions: NIR_{SRS} does not seem to be a valid technique to indirectly assess BAT in young healthy women. Further research is needed to validate this technique against other methods such as PET/CT using different radiotracers or magnetic resonance imaging.

Key words: Acute cold exposure, BAT perfusion, Cold-induced thermogenesis, Energy balance, Molecular imaging, Oxygen consumption, Oxygen delivery

Francisco M. Acosta and Jörn Berchem contributed equally to this work.

Electronic supplementary material The online version of this article (https://doi.org/10.1007/s11307-018-1244-5) contains supplementary material, which is available to authorized users.

Correspondence to: Francisco Acosta; *e-mail:* acostaf@ugr.es

Introduction

Brown adipose tissue (BAT) is a thermogenic tissue regulated by the sympathetic nervous system that defends core body temperature when mammals are exposed to temperatures below thermoneutrality [1]. It is able to oxidise glucose and lipids and dissipate energy in the form of heat [1–3]. Human BAT is mainly located in the supraclavicular region [4–7], and it seems to have an important role in the regulation of energy metabolism and whole-body insulin sensitivity in humans [1, 8].

To date, 2-deoxy-2-[^{18}F]fluoro-D-glucose ([^{18}F]DG) positron emission tomography combined with X-ray computed tomography (PET/CT) is the most frequently used technique to quantify human BAT volume and activity. However, this technique has several limitations, such as the exposure to ionising radiation and its high cost. More importantly, this technique is likely to underestimate BAT activity, since it only measures glucose uptake and BAT mainly takes up intracellular triglycerides [9–12]. Therefore, a new technique to estimate human BAT volume and activity with fewer limitations than [^{18}F]DG-PET/CT is needed [13, 14].

Near-infrared spatially resolved spectroscopy (NIR_{SRS}) is a simple, non-expensive, and non-invasive method to measure tissue oxygenation *in vivo* [15]. NIR_{SRS} measures different optical properties of the tissue based on oxygen-dependent absorption changes [16], and it allows to calculate the tissue saturation index (TSI) and the concentrations of total haemoglobin (tHb), oxy-haemoglobin (O_2Hb), and deoxy-haemoglobin (HHb). The TSI reflects the balance between oxygen delivery and consumption [17–19], and tHb has been used as an index of blood volume and tissue vascular innervation [16, 17]. BAT is highly vascularised, it presents a high mitochondrial density, and it shows an increased oxygen consumption and oxygen delivery when it is activated by cold [19–24]. Hence, NIR_{SRS} should be able to indirectly assess BAT volume and/or activity.

Nirengi et al. [22] showed, for the first time, that near-infrared time-resolved spectroscopy (NIR_{TRS}) parameters [scattering coefficient (as a proxy of mitochondrial density) and tHb] were positively correlated with BAT activity estimated by [^{18}F]DG-PET/CT in young males. Moreover, they suggested that NIR_{TRS} parameters were able to discriminate the presence of BAT with high sensitivity, specificity, and accuracy [25]. However, it remains unknown whether these findings apply to women (who present different physiological responses to acute cold and higher relative levels of BAT) [4] and whether they are replicated with other NIRS devices.

Recently, an expert panel recommended the use of an individualised cooling protocol before the [^{18}F]DG-PET/CT scan, as well as applying a standardised uptake value (SUV) threshold individualised to lean body mass and a Hounsfield units (HU) range between − 190 and − 10 to quantify BAT. Of note is that the cooling protocol that Nirengi et al. [22] applied was not individualised (2 h of cold exposure at 19 °C, intermittently placing the participants' feet on ice blocks), and that the SUV threshold was not relative to lean body mass [26].

Consequently, we aimed to examine the association of the NIR_{SRS} parameters (TSI, tHb, O_2Hb, and HHb) measured in the supraclavicular and forearm regions with BAT volume and activity (SUV_{mean} and SUV_{peak}) estimated by [^{18}F]DG-PET/CT in young healthy women, following the current recommendations.

Materials and Methods

Study Participants

A total of 18 Caucasian young women (age, 22 ± 2 years old) participated in this study [27]. All participants were healthy and non-smokers and did not take any medication that could have altered their cardiovascular or thermoregulatory responses to cold exposure. The study protocol and written informed consent were performed in accordance with the Declaration of Helsinki (revision of 2013). The study was approved by the Ethics Committee on Human Research of the University of Granada (n° 924) and of the Servicio Andaluz de Salud (Centro de Granada, CEI-Granada).

Procedures

Personalised Cold Exposure Before PET/CT Measurements

The study protocol is shown in Fig. 1. The participants arrived at the lab and confirmed having met the pre-study conditions: arriving in fasting state (at least 6 h), having slept as usual, having refrained from any moderate (within 24 h) or vigorous (within 48 h) physical activity, and not having consumed any alcoholic or stimulant beverages (within 6 h) or drugs which could have affected the peripheral circulation (within 24 h). Then, they voided their bladders and dressed in standardised clothes. The participants stayed in a warm room (22–23 °C) for 30 min in order to acclimatise. During this time, 2 NIR_{SRS} devices (Portamon, Artinis Medical Systems, the Netherlands) were attached to the participants: one device was attached to the *fossa supraclavicular major* on the left side of the body (Fig. S1A, Electronic Supplementary Material (ESM)), whereas the other one was attached to the left ventral forearm, in the midpoint between the *regio cubitalis anterior* and the *articulatio carpi* (Fig. S1B, ESM). Both devices were covered with black neoprene cloths to avoid environmental light. Then, a baseline measurement of the NIR_{SRS} parameters was taken in warm conditions during 10 min.

After that, the participants underwent a 2-h personalised cold exposure [28], during which the NIR_{SRS} parameters were continuously recorded. Briefly, the participants entered a cold room (19.5–20 °C) and wore a temperature-controlled water circulation cooling vest (Polar Products Inc., Ohio, USA) for 60 min set at ~4 °C above their shivering

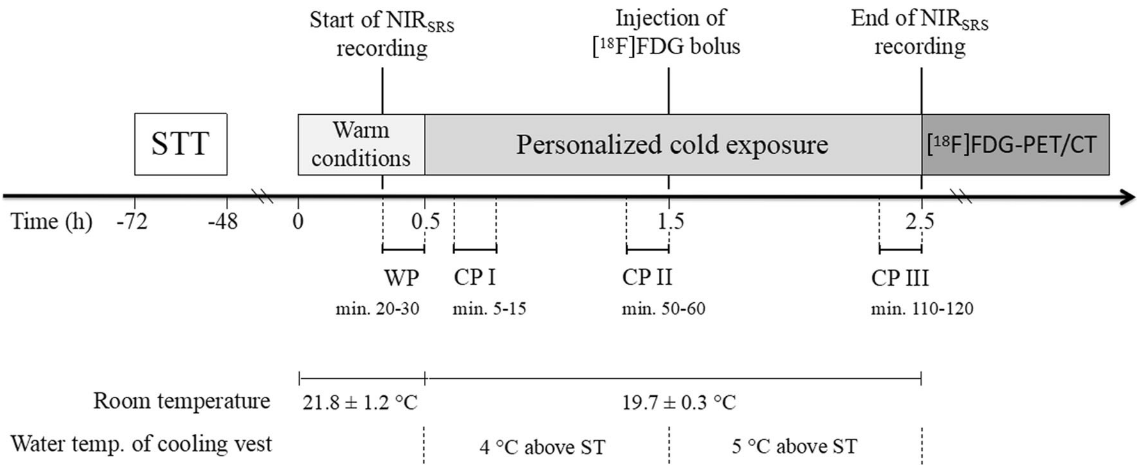

Fig. 1. Study protocol. The room temperature is provided as mean ± standard deviation. CP I: cold period I, CP II: cold period II, CP III: cold period III, [^{18}F]DG-PET/CT: 2-deoxy-2-[^{18}F]fluoro-D-glucose positron emission tomography combined with computed tomography, ST: shivering threshold, STT: shivering threshold test, WP: warm period.

threshold. The shivering threshold was defined as the water temperature at which shivering onset was self-reported by the participants and visually determined by the evaluators in a gradual cooling protocol performed 48–72 h prior to the PET/CT scan.

After 60 min of personalised cold exposure, we injected a bolus of [^{18}F]DG (180.6 ± 5.8 MBq ≈ 2.9 MBq/kg) and raised the water temperature of the vest ~1 °C for the last 60 min to avoid shivering. During the personalised cold exposure, the participants were not allowed to talk, move, or rub their bodies. After the 2-h personalised cold exposure, the participants went into the PET/CT scan (Siemens Biograph 16 PET/CT, Siemens, Germany) (see Fig. 1). For the CT acquisition, a peak kilovoltage of 120 was applied, while a scan time of 6 min per bed position was set for the PET acquisition. In total, 2 bed positions were scanned, from the *atlas vertebrae* to the *thoracic vertebrae 6* [28].

Measurements

NIR_{SRS} Parameters We used a NIR_{SRS} device (Portamon, Artinis Medical Systems, the Netherlands), a dual-wavelength (760–850 nm) continuous system which simultaneously combines the modified Lambert-Beer law, and spatially resolved spectroscopy. The sampling frequency was set at 10 Hz, and a differential pathlength factor of 4 was chosen for the supraclavicular and forearm regions. To note is that Portamon light sources were located at 30, 35, and 40 mm from the receiver, assuming a penetration depth of approximately 2 cm and a measurement of approximately 4 cm^3 [29].

The NIR_{SRS} data were analysed with Oxysoft software (Portamon, Artinis Medical Systems, the Netherlands) during 4 different periods: (i) warm period (WP), which comprised the 10-min record in warm conditions; (ii) cold period I (CP I), from 5 to 15 min; (iii) cold period II (CP II), from 50 to 60 min; and (iv) cold period III (CP III), from 110 to 120 min of the personalised cold exposure prior to the PET/CT scan. We obtained the TSI expressed as percentages as well as the concentrations of tHb, O_2Hb, and HHb, expressed in micromolar units (μM). The TSI was calculated as $O_2Hb/(O_2Hb + HHb) \times 100$, and tHb as $O_2Hb + HHb$ [30]. We additionally calculated (i) the area under the curve (AUC) following the trapezoidal rule, in order to analyse the overall change of the NIR_{SRS} parameters through cold exposure; and (ii) the cold-induced changes in the NIR_{SRS} parameters from the baseline to CP I, CP II, and CP III (expressed as percentages).

BAT Parameters Estimated by [^{18}F]DG-PET/CT PET/CT scans were analysed using software based on Beth Israel plugin for FIJI http://sourceforge.net/projects/bifijiplugins/ [31]. We calculated the standardised uptake value (SUV) as [^{18}F]DG uptake (kBq/ml)/(injected dose [kBq]/patient weight [g]). The SUV threshold for a voxel to be considered BAT was calculated as SUV ≥ [1.2/ (lean body mass/body mass)], and a fixed range of HU (− 190 to − 10) was applied [26]. The region of interest (ROI) was outlined from the

Table 1. Characteristics of the participants, $n = 18$

Age (years)	21.9	(2.1)
Weight (kg)	62.2	(11.4)
Height (m)	1.6	(0.06)
BMI (kg/m^2)	23.1	(3.7)
Fat mass (kg)	23	(7)
Lean mass (kg)	36	(5.2)
SUV threshold (g/ml)	2.1	(0.2)
BAT volume (ml)	82.5	(38.9)
BAT SUV_{mean} (g/ml)	3.9	(1.2)
BAT SUV_{peak} (g/ml)	12	(5.4)
BAT metabolic activity (g)	336.4	(208)

Values are mean (standard deviation). *BMI* body mass index, *BAT* brown adipose tissue, *SUV* standardised uptake value

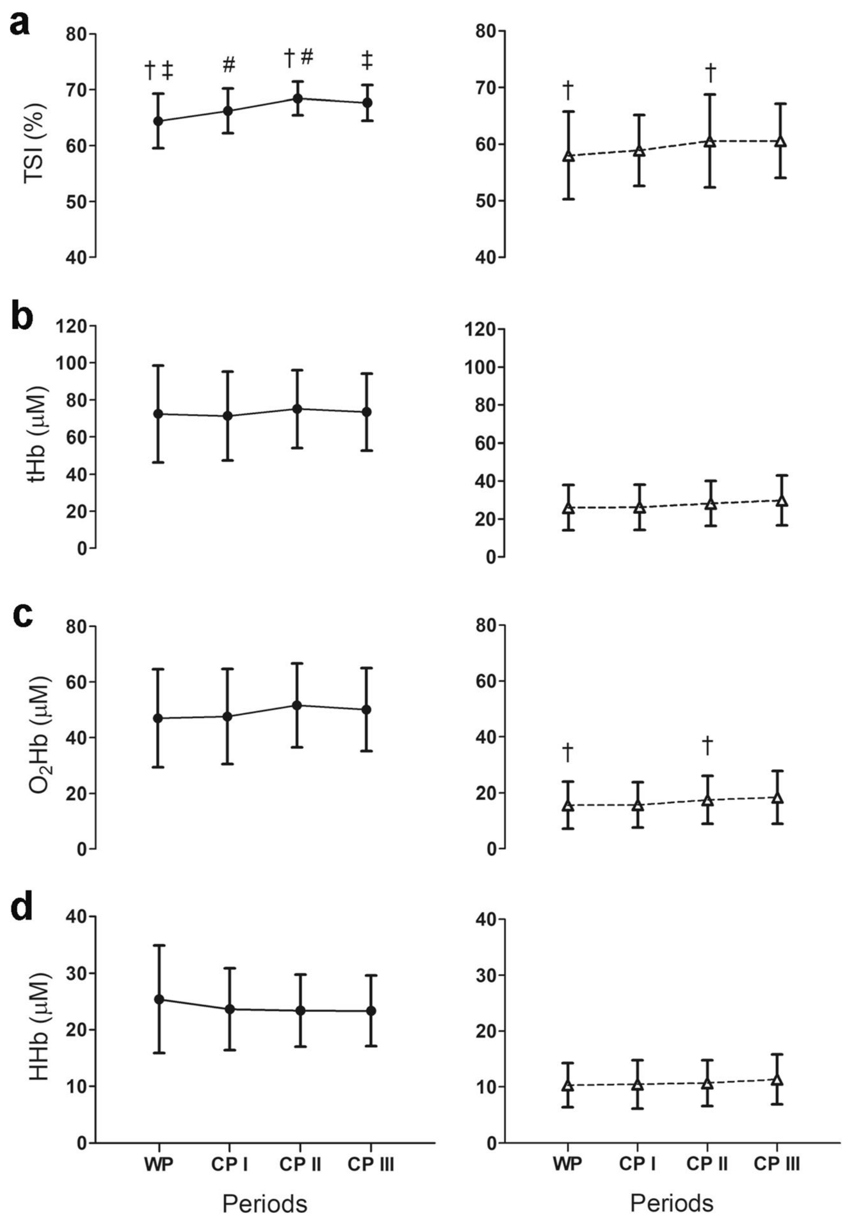

Fig. 2. **a** Tissue saturation index (TSI) and concentrations of **b** total haemoglobin (tHb), **c** oxy-haemoglobin (O_2Hb), and **d** deoxy-haemoglobin (HHb) across study periods. The measurements were taken in the left supraclavicular (●, solid line, $n = 16$) and forearm (▵, dashed line, $n = 17$) regions. Values are mean ± standard deviation. A repeated measures analysis of variance (ANOVA) was performed, using the Bonferroni post hoc test for pairwise comparisons. The symbols show significant differences between periods ($P < 0.05$). CP I: cold period I, CP II: cold period II, CP III: cold period III, WP: warm period.

atlas vertebrae to the *thoracic vertebrae* 4, and within this ROI, we estimated 3 BAT parameters to correlate with the NIR_{SRS} parameters: (i) total BAT volume (ml) as the amount of [^{18}F]DG uptake inside the ROI; (ii) SUV_{mean} as the average of pixels, which achieved the established criteria; (iii) SUV_{peak} as the highest average SUV in 1 ml spherical volume [26, 32]. Additionally, we calculated the BAT metabolic activity, as BAT volume*SUV_{mean}. PET/CT scans were visually and carefully examined to detect [^{18}F]DG uptake in BAT-specific depots (see Fig. S1C, D, and E (ESM)).

Body Composition The participants were weighed and their height was taken on a different day to the shivering threshold test and personalised cold exposure (Seca, Hamburg, Germany). We assessed the fat mass and lean body mass by a dual energy X-ray absorptiometry (DXA, HOLOGIC Wii).

Statistical Analysis

The changes in the TSI and in the concentrations of tHb, O_2Hb, and HHb in the supraclavicular and forearm regions through

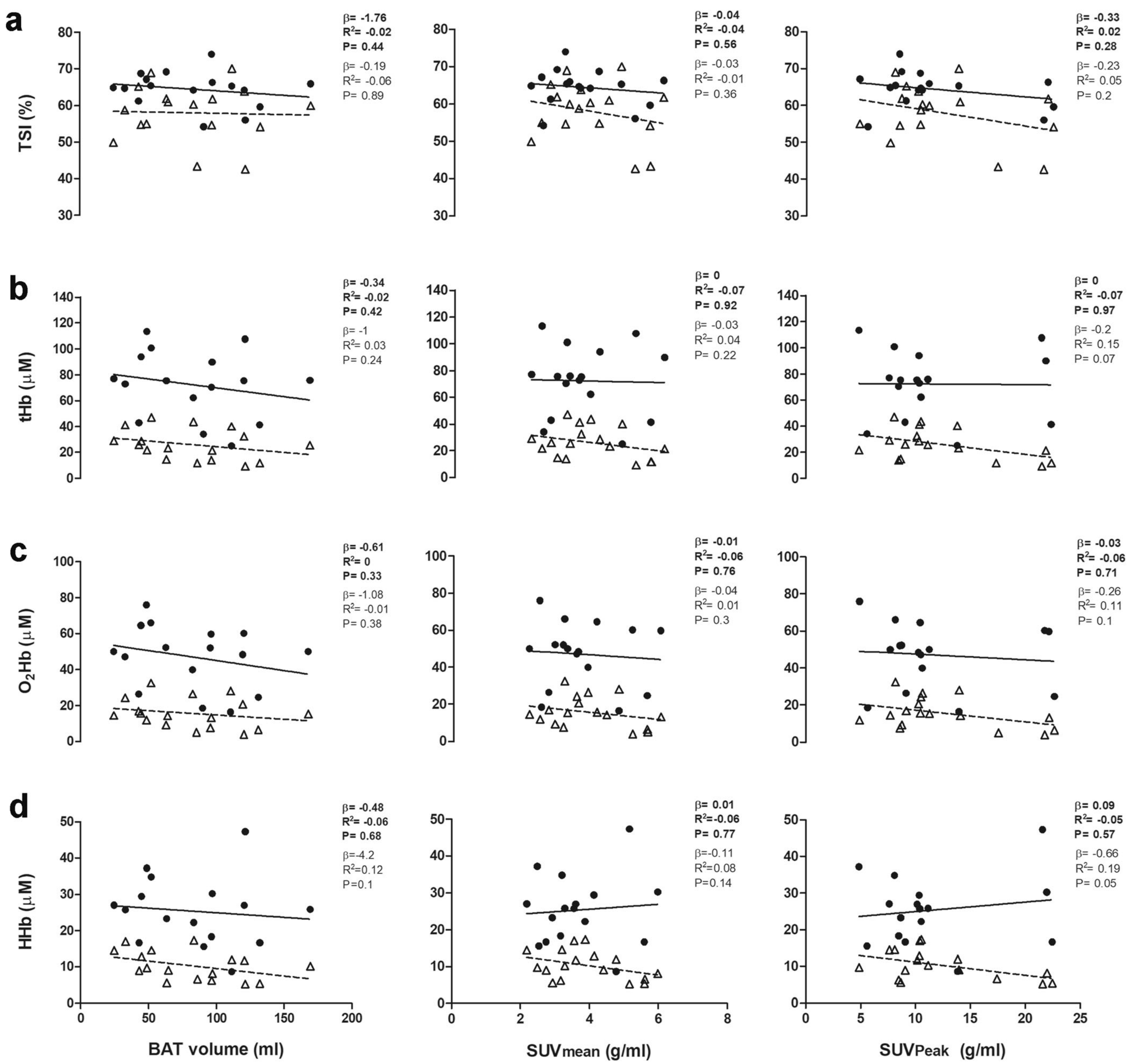

Fig. 3. Association of **a** tissue saturation index (TSI) and concentrations of **b** total haemoglobin (tHb), **c** oxy-haemoglobin (O_2Hb), and **d** deoxy-haemoglobin (HHb) measured in the supraclavicular (•, solid line: n = 16) and forearm regions (△, dashed line: n = 17) in warm conditions (WP) with BAT volume and activity (SUV_{mean} and SUV_{peak}) estimated by [^{18}F]DG-PET/CT. Non-standardised β coefficient, adjusted R^2, and P value are provided. BAT: brown adipose tissue, CP I: cold period I, CP II: cold period II, CP III: cold period III, HHb: deoxy-haemoglobin concentration, O_2Hb: oxy-haemoglobin concentration, tHb: total-haemoglobin concentration, SUV: standardised uptake value, TSI: tissue saturation index, WP: warm period.

cold exposure were analysed by a one-way repeated measures analysis of variance. We performed pairwise comparisons using the Bonferroni post hoc test. Linear regression analyses were firstly applied to examine the association between the NIR_{SRS} parameters in the supraclavicular and forearm regions in warm conditions (no previous cold exposure) and BAT volume and activity (SUV_{mean} and SUV_{peak}). Then, further linear regression analyses were performed to examine the association between the AUC- and cold-induced changes of the NIR_{SRS} parameters in the supraclavicular region and BAT volume and activity. The level of significance was set at $P < 0.05$. We conducted statistical analyses using the Statistical Package for the Social Sciences (SPSS version 24, Inc. Chicago, IL, USA).

Table 2. Association of the AUC of the NIR_{SRS} parameters in the supraclavicular region with BAT volume and activity (SUV_{mean} and SUV_{peak}) estimated by [^{18}F]DG-PET/CT, $n = 16$

	AUC (% baseline)	B	95%CI	β	P	Adj. R^2
BAT volume (ml)	TSI	2.25	(−2.39 , 6.89)	0.27	0.32	0.01
	tHb	0.59	(−0.98 , 2.16)	0.21	0.43	−0.02
	O_2Hb	0.56	(−0.70 , 1.82)	0.25	0.36	−0.01
	HHb	0.33	(−1.46 , 2.12)	0.11	0.70	−0.06
SUV_{mean} (g/ml)	TSI	0.03	(−0.10 , 0.16)	0.13	0.64	−0.05
	tHb	−0.02	(−0.06 , 0.03)	−0.23	0.40	−0.02
	O_2Hb	−0.01	(−0.05 , 0.03)	−0.18	0.52	−0.04
	HHb	−0.02	(−0.07 , 0.03)	−0.27	0.36	0.01
SUV_{peak} (g/ml)	TSI	0.23	(−0.41 , 0.87)	0.2	0.45	−0.03
	tHb	−0.09	(−0.31 , 0.12)	−0.25	0.36	−0.01
	O_2Hb	−0.05	(−0.23 , 0.12)	−0.17	0.52	−0.04
	HHb	−0.13	(−0.36 , 0.1)	−0.3	0.25	0.03

AUC area under the curve, *B* non-standardised regression coefficient, β standardised regression coefficient, *BAT* brown adipose tissue, *CI* confidence interval, *HHb* deoxy-haemoglobin concentration, NIR_{SRS} near-infrared spatially resolved spectroscopy, O_2Hb oxy-haemoglobin concentration, *tHb* total-haemoglobin concentration, *TSI* tissue saturation index

Results

Table 1 shows the characteristics of the participants. All participants included in the present study had positive uptake of glucose in the BAT-specific depots. We excluded the NIR_{SRS} measurements in the supraclavicular region of 2 participants and in the forearm region of 1 participant, due to technical problems.

NIR_{SRS} Parameters Along 2 h of Personalised Cold Exposure

The TSI significantly increased in the supraclavicular region from WP to CP II [mean difference (95 % confidence interval) 4.03 % (6.67, 1.39), $P = 0.02$] and CP III [3.26 % (5.81, 0.7), $P = 0.09$], as well as from CP I to CP II [2.2 % (4.31, 0.1), $P = 0.037$, Fig. 2]. The TSI showed the same trend in the forearm region, increasing from WP to CP II [2.56 % (4.95, 0.16), $P = 0.03$]. There was an increase in the concentration of O_2Hb in the forearm region from WP to CP II [1.88 µM (3.7, 0.06), $P = 0.04$], and CP III [2.76 µM (5.53, 0.01), $P = 0.05$], whereas no changes were observed in the supraclavicular region ($P > 0.05$, Fig. 2). No differences were observed in the concentrations of tHb and HHb along the cold exposure in neither the supraclavicular nor the forearm regions (all $P > 0.05$).

Relationship Between NIR_{SRS} Parameters and BAT Volume and Activity Estimated by [^{18}F]DG-PET/CT

There was no association between the NIR_{SRS} parameters in the supraclavicular region in warm conditions (WP) and BAT volume and activity (SUV_{mean} and SUV_{peak}) ($P > 0.05$) (Fig. 3). Similarly, the NIR_{SRS} parameters in the forearm region in warm conditions (WP) were not associated with BAT volume and SUV_{mean}. Nevertheless, the concentration of HHb in the forearm region was inversely associated with SUV_{peak} (non-standardised beta coefficient, adjusted R^2, P value $\beta = -0.66$, $R^2 = 0.19$, $P = 0.05$, Fig. 3). Moreover, we examined the relationship between the AUC- and cold-induced changes of the NIR_{SRS} parameters in the supraclavicular region with BAT volume and activity, and no significant associations were found ($P > 0.05$) (Table 2; Figs. 4, 5, and 6, respectively). To note is that the results remained similar when BAT volume and activity were calculated using different combinations of SUV thresholds and HU ranges: (i) SUV 2, HU −250 to −50; (ii) SUV 2, HU −300 to −10; and (iii) SUV 1.5, HU −180 to −10.

Discussion

This study shows that NIR_{SRS} does not seem to be a valid technique to indirectly assess BAT in young healthy women. There was no association between the NIR_{SRS} parameters in the supraclavicular region in warm conditions (no previous cold exposure) and BAT volume and activity (SUV_{mean} and SUV_{peak}). Similarly, the AUC- and cold-induced changes of the NIR_{SRS} parameters in the supraclavicular region were not associated with BAT volume and activity.

NIR_{SRS} Parameters During 2 h of Personalised Cold Exposure

Several studies have shown that BAT oxidative metabolism increases after acute cold exposure and cold acclimation [9, 33]. In addition, BAT perfusion can be increased up to 1.5–2-fold after an acute cold exposure [19, 23], and it is positively associated with the metabolic rate of oxygen ($R^2 = 0.90$, $P = 0.01$) [19]. Since NIR_{SRS} parameters [TSI and tHb] have been shown as proxies of the balance between oxygen delivery and consumption, and of the blood volume and tissue vasculature [16–18], they may be able to indirectly assess BAT volume and activity.

We hypothesised that a decrease of the TSI and an increase in the concentration of tHb would occur in the

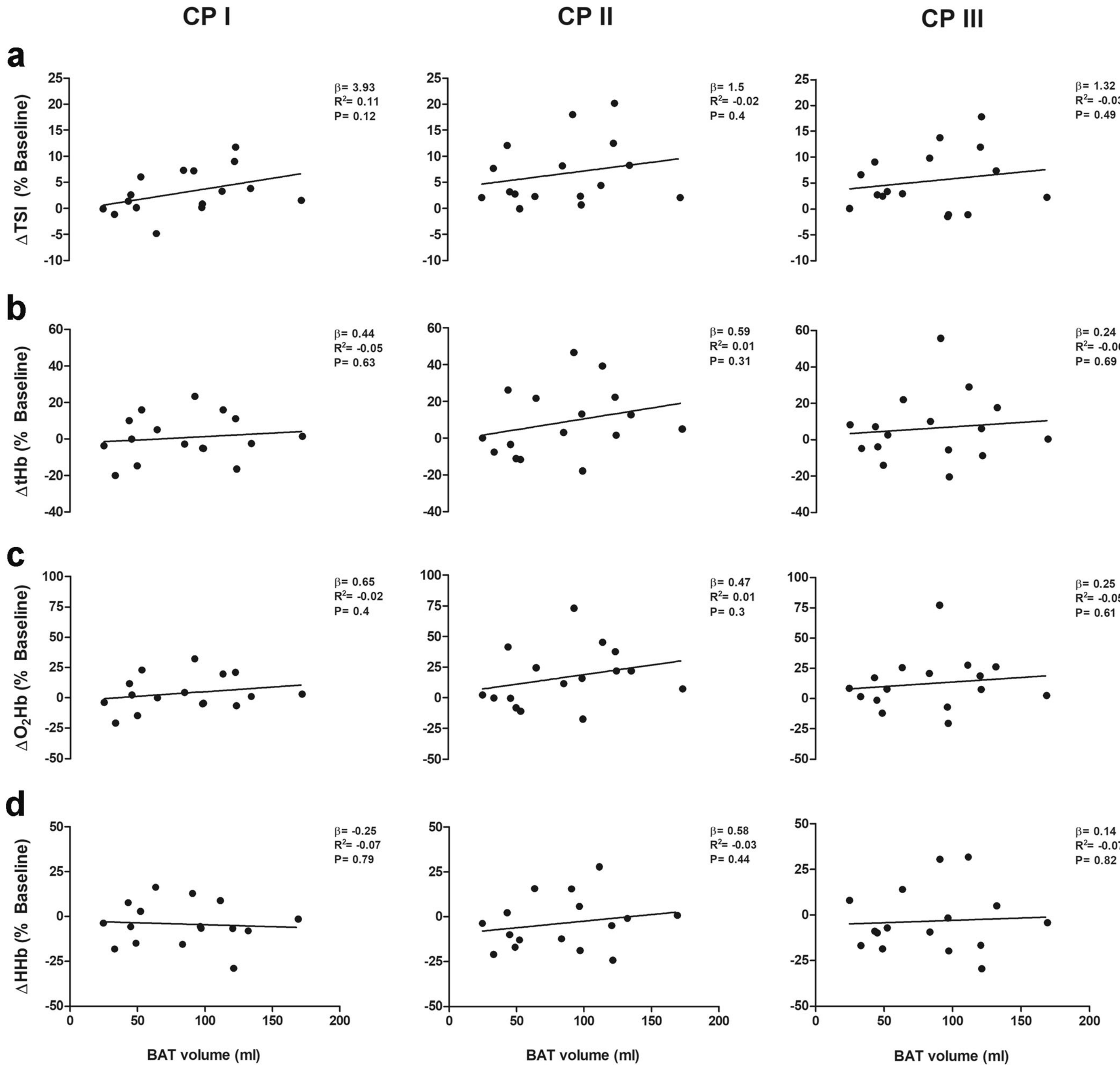

Fig. 4. Association of cold-induced changes in **a** tissue saturation index (TSI) and concentrations of **b** total haemoglobin (tHb), **c** oxy-haemoglobin (O_2Hb), and **d** deoxy-haemoglobin (HHb) with BAT volume estimated by [^{18}F]DG-PET/CT ($n = 16$). Cold-induced changes in the NIR_{SRS} parameters are calculated as differences from the warm period to CP I, CP II, and CP III (% baseline). A linear regression analysis was performed. Non-standardised β coefficient, adjusted R^2 squared and P value are provided. CP I: cold period I, CP II: cold period II, CP III: cold period III, HHb: deoxy-haemoglobin concentration, O_2Hb: oxy-haemoglobin concentration, tHb: total-haemoglobin concentration, TSI: tissue saturation index, WP: warm period.

supraclavicular region in response to a personalised cold exposure, indicating a higher BAT oxygen consumption and blood volume. Paradoxically, our results showed an increase of the TSI in the supraclavicular region after 1 and 2 h of personalised cold exposure, which indicated an increase in the tissue oxygenation. These results may be explained by the influence of the superficial skin layer. An inherent limitation in NIRS is that this technique is not able to measure haemodynamic changes in isolated tissues (such as BAT), measuring the multilayer and inhomogeneous tissue characteristics of the supraclavicular region, composed by the skin, adipose tissue, and muscle (among other tissues). Davis et al. [34] showed that continuous wave NIRS measurements of tissue oxygenation could be potentially affected by the skin blood flow, especially during conditions where both skin and muscle blood flows are elevated

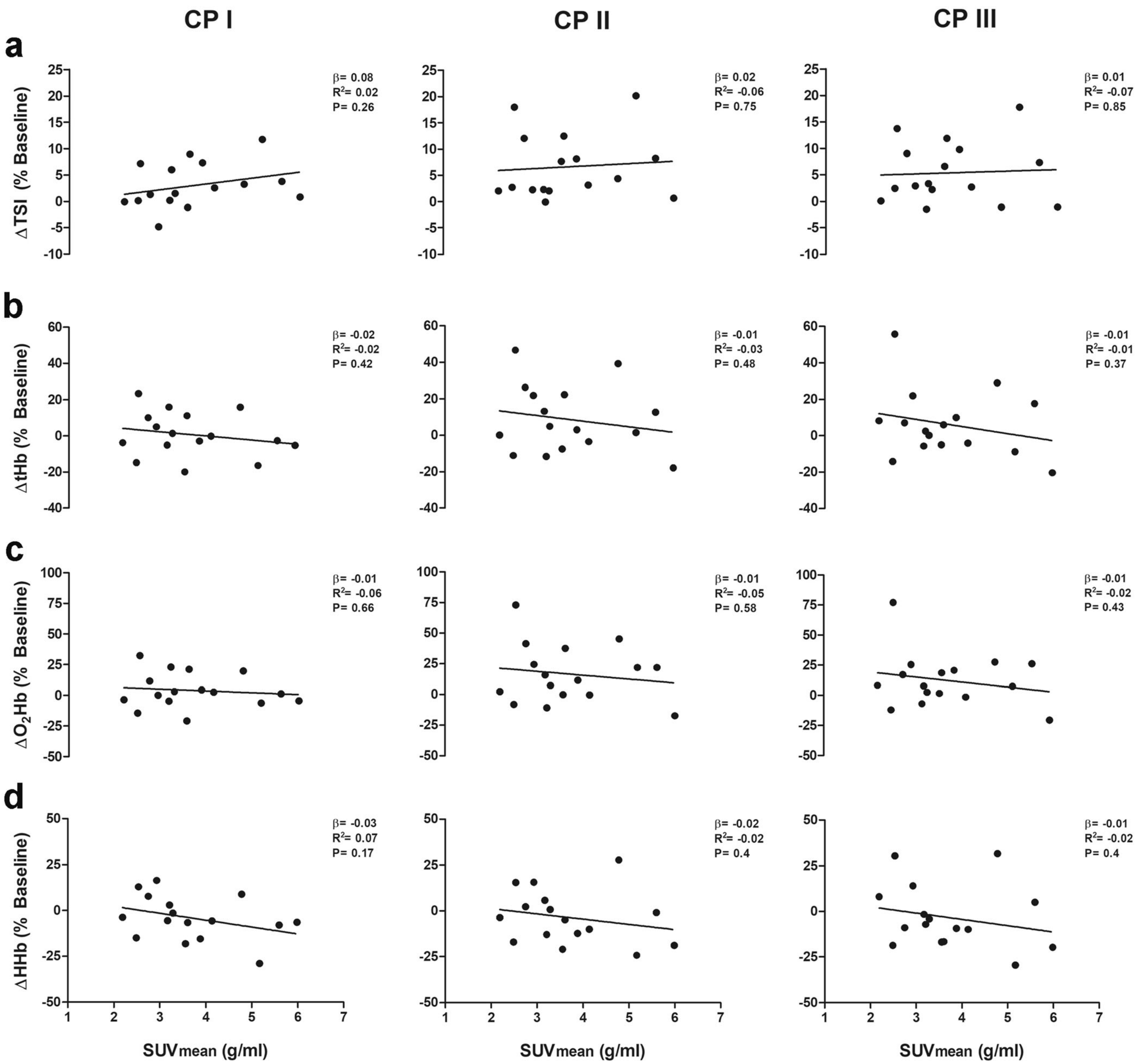

Fig. 5. Association of cold-induced changes in **a** tissue saturation index (TSI) and concentrations of **b** total haemoglobin (tHb), **c** oxy-haemoglobin (O_2Hb), and **d** deoxy-haemoglobin (HHb) with SUV_{mean} estimated by [^{18}F]DG-PET/CT ($n = 16$). Cold-induced changes in the NIR_{SRS} parameters are calculated as differences from the warm period to CP I, CP II, and CP III (% baseline). A linear regression analysis was performed. Non-standardised β coefficient, adjusted R^2, and P value are provided. CP I: cold period I, CP II: cold period II, CP III: cold period III, HHb: deoxy-haemoglobin concentration, O_2Hb: oxy-haemoglobin concentration, tHb: total-haemoglobin concentration, SUV: standardised uptake value, TSI: tissue saturation index, WP: warm period.

concomitantly (*e.g.*, doing exercise) [35], and might also extrapolate to cold. In addition, measurements of continuous wave NIRS devices are affected by the assumption of a constant reduced scattering and differential pathlength factor [35, 36], and are more sensitive to the optical signals in the superficial layers (as skin) than NIR_{TRS} [37]. Cold exposure induces cutaneous vasoconstriction and a concomitant decrease in skin blood flow [38], which might have masked an increase in BAT vasodilation [22] and could partially explain the increase in the tissue oxygenation of the supraclavicular region.

The haemoglobin concentration in the supraclavicular region did not change during the personalised cold exposure, which concur with the results reported by Nirengi et al. [22]. The fact that no changes in haemoglobin concentration were observed in the supraclavicular region, where BAT depots

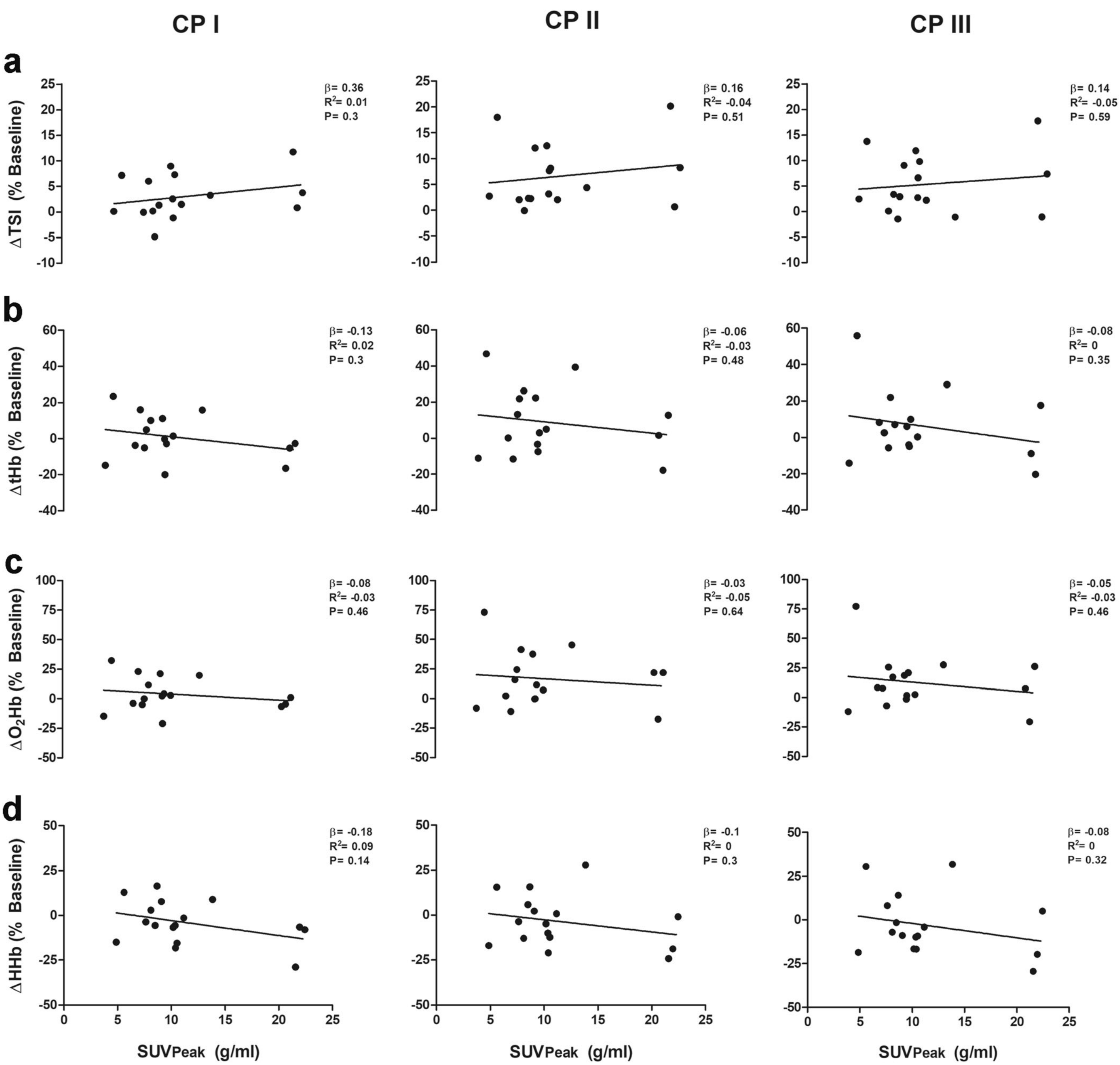

Fig. 6. Association of cold-induced changes in **a** tissue saturation index (TSI) and concentrations of **b** total haemoglobin (tHb), **c** oxy-haemoglobin (O_2Hb), and **d** deoxy-haemoglobin (HHb) with SUV$_{peak}$ estimated by [^{18}F]DG-PET/CT ($n = 16$). Cold-induced changes in the NIR$_{SRS}$ parameters are calculated as differences from the warm period to CP I, CP II, and CP III (% baseline). A linear regression analysis was performed. Non-standardised β coefficient, adjusted R^2, and P value are provided. CP I: cold period I, CP II: cold period II, CP III: cold period III, HHb: deoxy-haemoglobin concentration, O_2Hb: oxy-haemoglobin concentration, tHb: total-haemoglobin concentration, SUV: standardised uptake value, TSI: tissue saturation index, WP: warm period.

are mainly located and activated after an acute cold exposure [7, 39], might be explained by the superficial skin layer influence and the underestimation of BAT perfusion. Such underestimation could occur because concentrations of tHb, O_2Hb, and HHb measured by NIRS are sensitive to changes in blood volume, but not to perfusion flow velocity during high metabolic activities [22, 36, 40].

NIR$_{SRS}$ as an Indirect Technique to Assess Brown Adipose Tissue in Young Women

Previous evidence suggests that NIRS may be a valid technique to indirectly assess human BAT in cold conditions [19, 22, 25]. In fact, Nirengi et al. [22] proposed that NIR$_{TRS}$ parameters [scattering coefficient (as a proxy of mitochondrial density) and tHb] were capable of assessing BAT density at thermoneutral conditions (27 °C).

Contrary to Nirengi et al. [22], our results showed that NIR_{SRS} parameters in the supraclavicular region during warm conditions (WP) were not associated with BAT activity (SUV_{mean} and SUV_{peak}) (all $P > 0.05$). Furthermore, we examined whether the AUC- and cold-induced changes of NIR_{SRS} parameters in the supraclavicular region were associated with BAT volume and activity, and we did not find any significant association. These differences could be based on (i) the characteristics of the devices, which may be the most influencing factor (Nirengi et al. used a NIR_{TRS} device, whereas we used a NIR_{SRS} device). Furthermore, the lack of studies determining the validity and comparison of both techniques when examining haemodynamic changes hampers the understanding of results from different studies. (ii) Women present different physiological responses to acute cold than men as well as higher levels of BAT [^{18}F]DG uptake activity [4]. (iii) The use of a different cooling protocol: while Nirengi et al. [22] applied a fixed cooling protocol, we applied a personalised cold exposure in order to maximise BAT activation [26, 41]. Finally, to mention is that participants from our study presented a greater mean and lower standard deviation in SUV_{mean} compared to those of Nirengi et al. [22] (3.9 ± 1.2 *vs.* 2.7 ± 2.2 g/ml, respectively), which may have affected the association between the NIR_{SRS} parameters and BAT activity.

Limitations

A limitation to consider in the present study is the assumption of the reduced scattering coefficient and differential pathlength factor as constant, which may have affected NIR_{SRS} measurements [35]. The *in vivo* scattering properties of the biological tissues, the unknown contribution of myoglobin to the signal, and the impossibility to measure specific tissues are inherent limitations in NIRS. The fact that NIRS signal is also influenced by potential confounders should be considered [42–44]. Of note is that [^{18}F]DG-PET/CT might be likely to underestimate BAT activity because it only measures glucose uptake, whereas BAT mainly takes up intracellular triglycerides [9–12]. Therefore, further research should be performed in order to validate NIR_{SRS} with PET/CT using other radiotracers (*e.g.*, [^{11}C]acetate, [^{18}F]FTHA or [^{11}C]palmitate) [45] or other techniques such as magnetic resonance imaging, to assess human BAT [46].

Conclusions

This study shows that NIR_{SRS} does not seem to be a valid technique to indirectly assess BAT in young healthy women. More studies are needed to verify whether NIRS can be used as a simple, complementary, and non-invasive technique when assessing human BAT. Nevertheless, these studies should compare NIRS techniques in different populations (*e.g.*, older, obese or diabetic participants), or with a different method than [^{18}F]DG-PET/CT.

Acknowledgments. We are grateful to Ms. Carmen Sainz-Quinn for the assistance with the English language and to Marco Dat (Artinis Medical Systems) for his excellent technical assistance.

Financial Support. The study was supported by the Spanish Ministry of Economy and Competitiveness (PTA 12264-I), Fondo de Investigación Sanitaria del Instituto de Salud Carlos III (PI13/01393), and Retos de la Sociedad (DEP2016-79512-R), Fondos Estructurales de la Unión Europea (FEDER), by the Spanish Ministry of Education (FPU 13/04365 and 15/04059), by the Fundación Iberoamericana de Nutrición (FINUT), by the Redes temáticas de investigación cooperativa RETIC (Red SAMID RD16/0022), by AstraZeneca HealthCare Foundation, and by the University of Granada, Plan Propio de Investigación 2016, Excellence actions: Units of Excellence; Unit of Excellence on Exercise and Health (UCEES). This study is part of a PhD thesis conducted in the Biomedicine Doctoral Studies, University of Granada, Spain.

Compliance with Ethical Standards

Conflict of Interest

The authors declare that they have no conflict of interest.

Ethical Approval

All procedures performed in studies involving human participants were in accordance with the ethical standards of the institutional and/or national research committee and with the 1964 Helsinki declaration and its later amendments or comparable ethical standards.

Informed Consent

Informed consent was obtained from all individual participants included in the study.

References

1. Cannon B, Nedergaard J (2004) Brown adipose tissue: function and physiological significance. Physiol Rev 84:277–359
2. Peirce V, Vidal-Puig A (2013) Regulation of glucose homoeostasis by brown adipose tissue. Lancet Diabetes Endocrinol 1:353–360
3. Schilperoort M, Hoeke G, Kooijman S, Rensen PCN (2016) Relevance of lipid metabolism for brown fat visualization and quantification. Curr Opin Lipidol 27:242–248
4. Cypess AM, Lehman S, Williams G, Tal I, Rodman D, Goldfine AB, Kuo FC, Palmer EL, Tseng YH, Doria A, Kolodny GM, Kahn CR (2009) Identification and importance of brown adipose tissue in adult humans. N Engl J Med 360:1509–1517
5. van Marken Lichtenbelt WD, Vanhommerig JW, Smulders NM, Drossaerts JMAFL, Kemerink GJ, Bouvy ND, Schrauwen P, Teule GJJ (2009) Cold-activated brown adipose tissue in healthy men. N Engl J Med 360:1500–1508
6. Virtanen KAK, Lidell MME, Orava J et al (2009) Functional brown adipose tissue in healthy adults. N Engl J Med 360:1518–1525
7. Leitner BP, Huang S, Brychta RJ, Duckworth CJ, Baskin AS, McGehee S, Tal I, Dieckmann W, Gupta G, Kolodny GM, Pacak K, Herscovitch P, Cypess AM, Chen KY (2017) Mapping of human brown adipose tissue in lean and obese young men. Proc Natl Acad Sci U S A 114:8649–8654
8. Lee P, Smith S, Linderman J, Courville AB, Brychta RJ, Dieckmann W, Werner CD, Chen KY, Celi FS (2014) Temperature-acclimated brown adipose tissue modulates insulin sensitivity in humans. Diabetes 63:3686–3698
9. Ouellet V, Labbé SM, Blondin DP, Phoenix S, Guérin B, Haman F, Turcotte EE, Richard D, Carpentier AC (2012) Brown adipose tissue oxidative metabolism contributes to energy expenditure during cold exposure in humans. J Clin Invest 122:545–552

10. Blondin DP, Labbé SM, Phoenix S, Guérin B, Turcotte ÉE, Richard D, Carpentier AC, Haman F (2015) Contributions of white and brown adipose tissues and skeletal muscles to acute cold-induced metabolic responses in healthy men. J Physiol 593:701–714
11. Blondin DP, Frisch F, Phoenix S, Guérin B, Turcotte ÉE, Haman F, Richard D, Carpentier AC (2017) Inhibition of intracellular triglyceride lipolysis suppresses cold-induced brown adipose tissue metabolism and increases shivering in humans. Cell Metab 25:438–447
12. Blondin DP, Tingelstad HC, Noll C, Frisch F, Phoenix S, Guérin B, Turcotte ÉE, Richard D, Haman F, Carpentier AC (2017) Dietary fatty acid metabolism of brown adipose tissue in cold-acclimated men. Nat Commun 8:14146
13. Liu X, Cervantes C, Liu F (2017) Common and distinct regulation of human and mouse brown and beige adipose tissues: a promising therapeutic target for obesity. Protein Cell 8:446–454
14. Cypess AM, Haft CR, Laughlin MR, Hu HH (2014) Brown fat in humans: consensus points and experimental guidelines. Cell Metab 20:408–415
15. Jobsis FF (1977) Noninvasive, infrared monitoring of cerebral and myocardial oxygen sufficiency and circulatory parameters. Science 198:1264–1267
16. Hamaoka T, McCully KK, Quaresima V et al (2007) Near-infrared spectroscopy/imaging for monitoring muscle oxygenation and oxidative metabolism in healthy and diseased humans. J Biomed Opt 12:062105
17. Boushel R, Langberg H, Olesen J, Gonzales-Alonzo J, Bulow J, Kjaer M (2001) Monitoring tissue oxygen availability with near infrared spectroscopy (NIRS) in health and disease. Scand J Med Sci Sports 11:213–222
18. Ferrari M, Muthalib M, Quaresima V (2011) The use of near-infrared spectroscopy in understanding skeletal muscle physiology: recent developments. Philos Trans R Soc 369:4577–4590
19. Muzik O, Mangner TJ, Leonard WR, Kumar A, Janisse J, Granneman JG (2013) ^{15}O PET measurement of blood flow and oxygen consumption in cold-activated human brown fat. J Nucl Med 54:523–531
20. u Din M, Raiko J, Saari T, Kudomi N, Tolvanen T, Oikonen V, Teuho J, Sipilä HT, Savisto N, Parkkola R, Nuutila P, Virtanen KA (2016) Human brown adipose tissue $[^{15}O]O_2$ PET imaging in the presence and absence of cold stimulus. Eur J Nucl Med Mol Imaging 43:1878–1886
21. Cinti S (2009) Transdifferentiation properties of adipocytes in the adipose organ. Am J Physiol Endocrinol Metab 297:E977–E986
22. Nirengi S, Yoneshiro T, Sugie H, Saito M, Hamaoka T (2015) Human brown adipose tissue assessed by simple, noninvasive near-infrared time-resolved spectroscopy. Obesity 23:973–980
23. Orava J, Nuutila P, Lidell MEE et al (2011) Different metabolic responses of human brown adipose tissue to activation by cold and insulin. Cell Metab 14:272–279
24. Khanna A, Branca RT (2012) Detecting brown adipose tissue activity with BOLD MRI in mice. Magn Reson Med 68:1285–1290
25. Nirengi S, Yoneshiro T, Saiki T et al (2016) Evaluation of brown adipose tissue using near-infrared time-resolved spectroscopy. In: Elwell CE, Leung TS, Harrison DK (eds) Oxygen Transport to Tissue XXXVII. Springer, New York, pp 371–376
26. Chen KY, Cypess AM, Laughlin MR, Haft CR, Hu HH, Bredella MA, Enerbäck S, Kinahan PE, Lichtenbelt WM, Lin FI, Sunderland JJ, Virtanen KA, Wahl RL (2016) Brown adipose reporting criteria in imaging STUDIES (BARCIST 1.0): recommendations for standardized FDG-PET/CT experiments in humans. Cell Metab 24:210–222
27. Sanchez-Delgado G, Martinez-Tellez B, Olza J et al (2015) Activating brown adipose tissue through exercise (ACTIBATE) in young adults: rationale, design and methodology. Contemp Clin Trials 45:416–425
28. Martinez-Tellez B, Sanchez-Delgado G, Garcia-Rivero Y et al (2017) A new personalized cooling protocol to activate brown adipose tissue in young adults. Front Physiol. https://doi.org/10.3389/fphys.2017.00863
29. Chance B, Nioka S, Kent J et al (1989) Time-resolved spectroscopy of hemoglobin and myoglobin in resting and ischemic muscle. Anal Biochem 174:698–707
30. Suzuki S, Takasaki S, Ozaki T, Kobayashi Y (1999) Tissue oxygenation monitor using NIR spatially resolved spectroscopy. Proc SPIE. https://doi.org/10.1117/12.356862
31. Schindelin J, Arganda-Carreras I, Frise E, Kaynig V, Longair M, Pietzsch T, Preibisch S, Rueden C, Saalfeld S, Schmid B, Tinevez JY, White DJ, Hartenstein V, Eliceiri K, Tomancak P, Cardona A (2012) Fiji: an open-source platform for biological-image analysis. Nat Methods 9:676–682
32. Hasenclever D, Kurch L, Mauz-Körholz C, Elsner A, Georgi T, Wallace H, Landman-Parker J, Moryl-Bujakowska A, Cepelová M, Karlén J, Álvarez Fernández-Teijeiro A, Attarbaschi A, Fosså A, Pears J, Hraskova A, Bergsträsser E, Beishuizen A, Uyttebroeck A, Schomerus E, Sabri O, Körholz D, Kluge R (2014) qPET—a quantitative extension of the Deauville scale to assess response in interim FDG-PET scans in lymphoma. Eur J Nucl Med Mol Imaging 41:1301–1308
33. Blondin DP, Labbe SM, Tingelstad HC et al (2014) Increased brown adipose tissue oxidative capacity in cold-acclimated humans. J Clin Endocrinol Metab 99:1027–1036
34. Davis SL (2006) Skin blood flow influences near-infrared spectroscopy-derived measurements of tissue oxygenation during heat stress. J Appl Physiol 100:221–224
35. Koga S, Poole DC, Kondo N et al (2014) Effects of increased skin blood flow on muscle oxygenation/deoxygenation: comparison of time-resolved and continuous-wave near-infrared spectroscopy signals. Eur J Appl Physiol 115:335–343
36. Ferreira LF, Hueber DM, Barstow TJ (2007) Effects of assuming constant optical scattering on measurements of muscle oxygenation by near-infrared spectroscopy during exercise. J Appl Physiol 102:358–367
37. Sato C, Yamaguchi T, Seida M, Ota Y, Yu I, Iguchi Y, Nemoto M, Hoshi Y (2007) Intraoperative monitoring of depth-dependent hemoglobin concentration changes during carotid endarterectomy by time-resolved spectroscopy. Appl Opt 46:2785–2792
38. Charkoudian N (2003) Skin blood flow in adult human thermoregulation: how it works, when it does not, and why. Mayo Clin Proc 78:603–612
39. Sacks H, Symonds ME (2013) Anatomical locations of human brown adipose tissue: functional relevance and implications in obesity and type 2 diabetes. Diabetes 62:1783–1790
40. Boushel R, Saltin B (2013) Ex vivo measures of muscle mitochondrial capacity reveal quantitative limits of oxygen delivery by the circulation during exercise. Int J Biochem Cell Biol 45:68–75
41. van der Lans AAJJ, Wierts R, Vosselman MJ, Schrauwen P, Brans B, van Marken Lichtenbelt WD (2014) Cold-activated brown adipose tissue in human adults: methodological issues. Am J Physiol Regul Integr Comp Physiol 307:R103–R113
42. Fadel PJ, Keller DM, Watanabe H, Raven PB, Thomas GD (2004) Noninvasive assessment of sympathetic vasoconstriction in human and rodent skeletal muscle using near-infrared spectroscopy and Doppler ultrasound. J Appl Physiol 96:1323–1330
43. Engel PAK, Severinghaus JW, Munson E (1965) The influence of temperature and pH on the dissociation curve of oxyhemoglobin of human blood. Scand J Clin Lab Invest 17:515–523
44. Tew GA, Ruddock AD, Saxton JM (2010) Skin blood flow differentially affects near-infrared spectroscopy-derived measures of muscle oxygen saturation and blood volume at rest and during dynamic leg exercise. Eur J Appl Physiol 110:1083–1089
45. Paulus A, van Marken Lichtenbelt W, Bauwens M (2017) Brown adipose tissue and lipid metabolism imaging. Methods 130:105–113
46. Sun L, Yan J, Sun L, Velan SS, Leow MKS (2017) A synopsis of brown adipose tissue imaging modalities for clinical research. Diabetes Metab 43:401–410